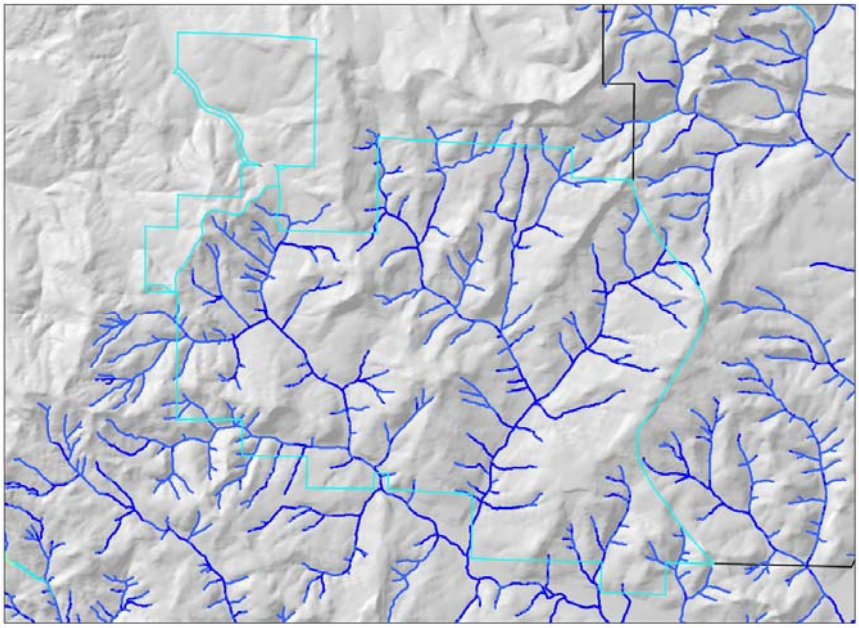

Figure D-26. Predicted debris flow probability for the Hamilton Management Basin. Refer to the Legend in Figure D-7. The predicted probabilities reflect cumulative landslide densities (that could trigger debris flows) and not individual pixel-based landslide potential shown in the landslide density map.

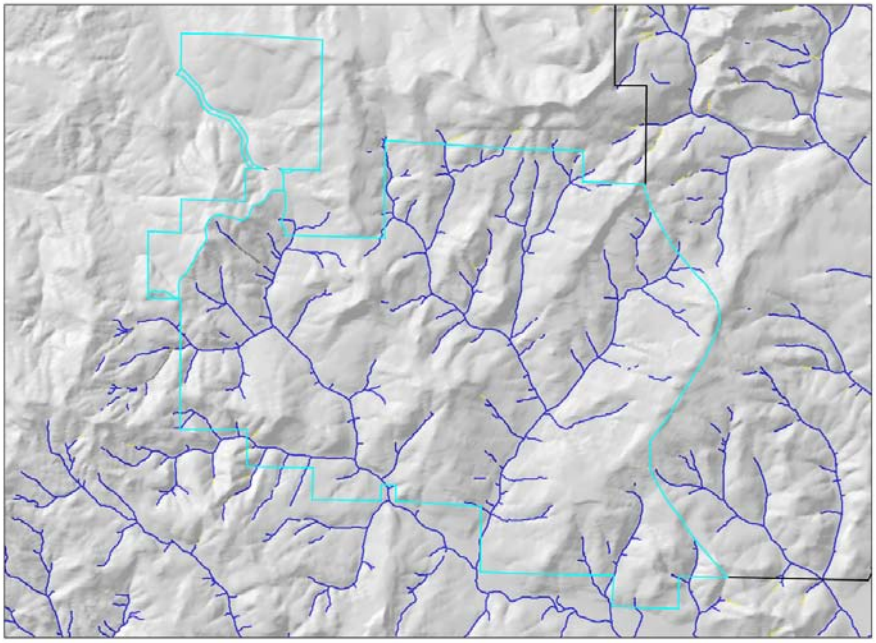

Figure D-27. Predicted headwater streams that contributed wood to fish-bearing channels by debris flows for the Hamilton Management Basin. Refer to the Legend in Figure D-7; predictions apply to headwater streams only. The predicted probabilities reflect cumulative landslide densities (that could trigger debris flows) and not individual pixel-based landslide potential shown in the landslide density map.

## 10. CRAWFORD MANAGEMENT BASIN

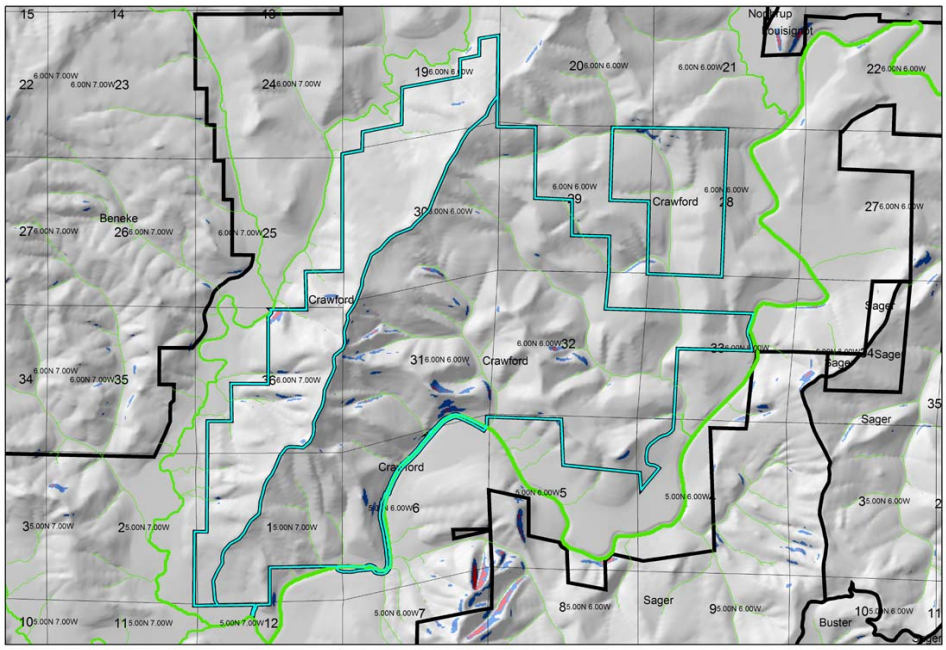


Figure D-28. Slope gradient map for the Crawford Management Basin. Refer to the Legend in Figure D-7.

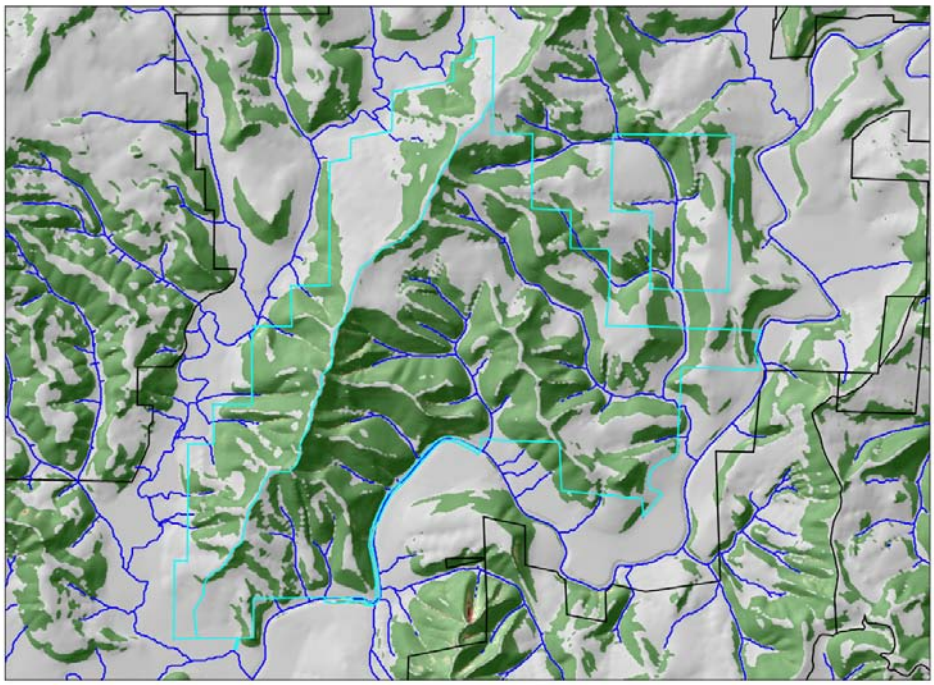

Figure D-29. Predicted landslide density for the Crawford Management Basin. Refer to the Legend in Figure D-7; the gray areas have no predicted landslide density.

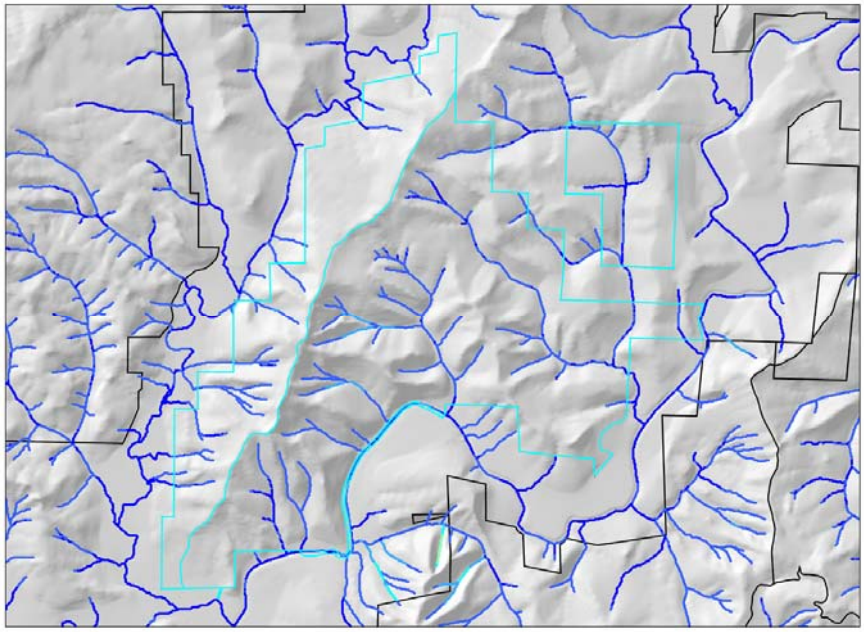

Figure D-30. Predicted debris flow probability for the Crawford Management Basin. Refer to the Legend in Figure D-7. The predicted probabilities reflect cumulative landslide densities (that could trigger debris flows) and not individual pixel-based landslide potential shown in the landslide density map.

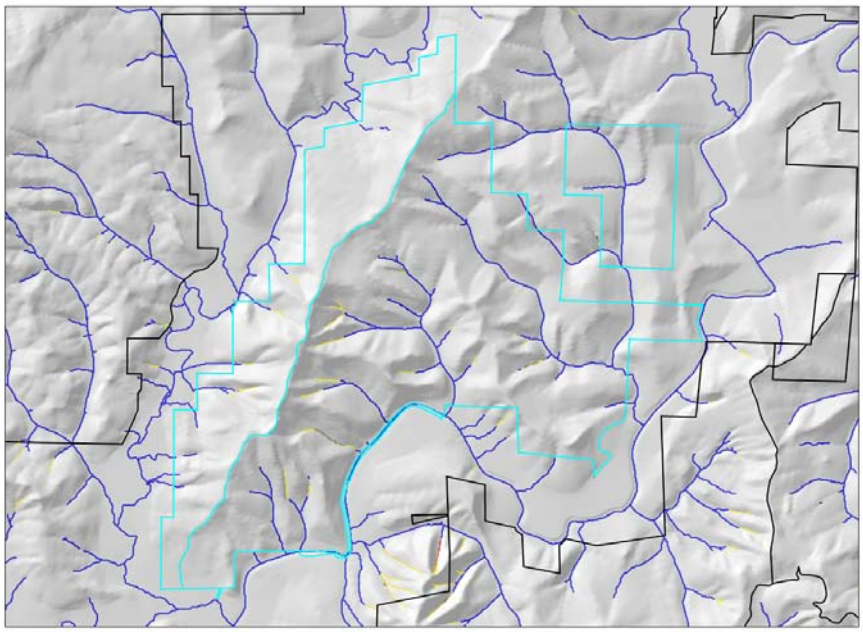

Figure D-31. Predicted headwater streams that contributed wood to fish-bearing channels by debris flows for the Crawford Management Basin. Refer to the Legend in Figure D-7; predictions apply to headwater streams only. The predicted probabilities reflect cumulative landslide densities (that could trigger debris flows) and not individual pixel-based landslide potential shown in the landslide density map.

## 11. SAGER MANAGEMENT BASIN

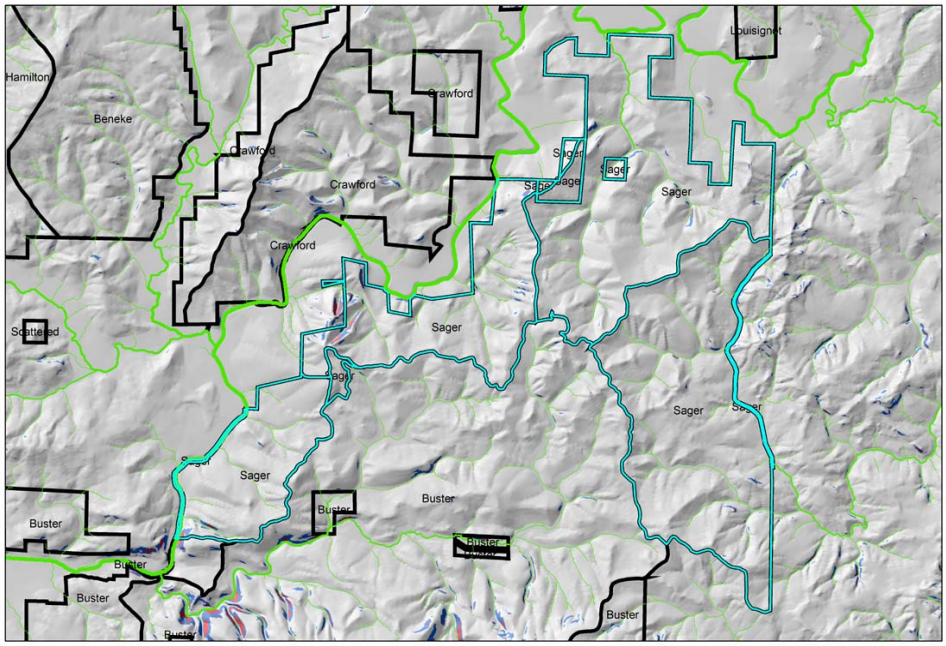


Figure D-32. Slope gradient map for the Sager Management Basin. Refer to the Legend in Figure D-7.

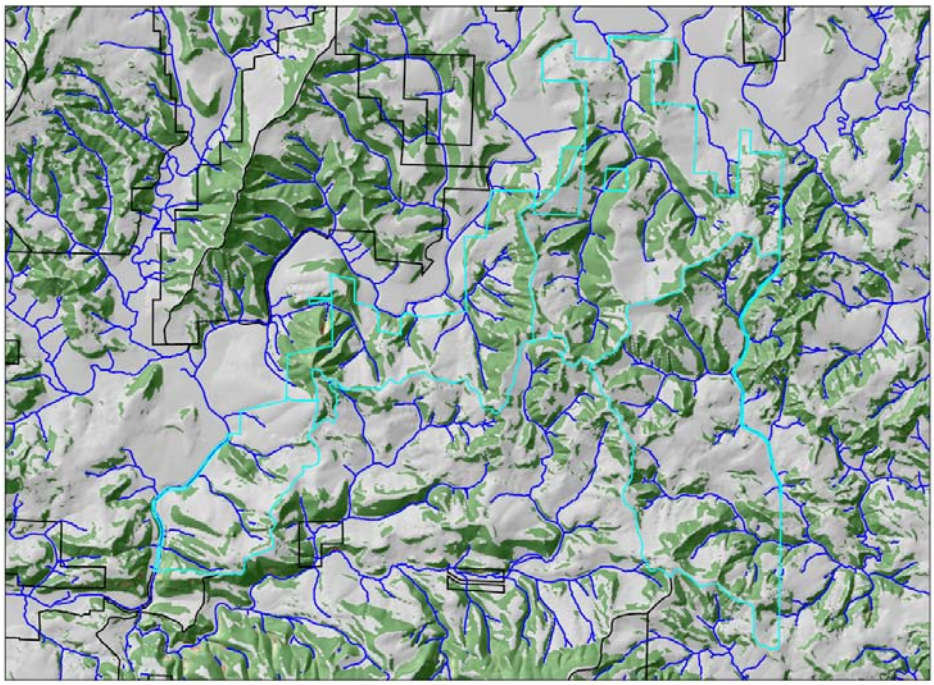

Figure D-33. Predicted landslide density for the Sager Management Basin. Refer to the Legend in Figure D-7; the gray areas have no predicted landslide density.

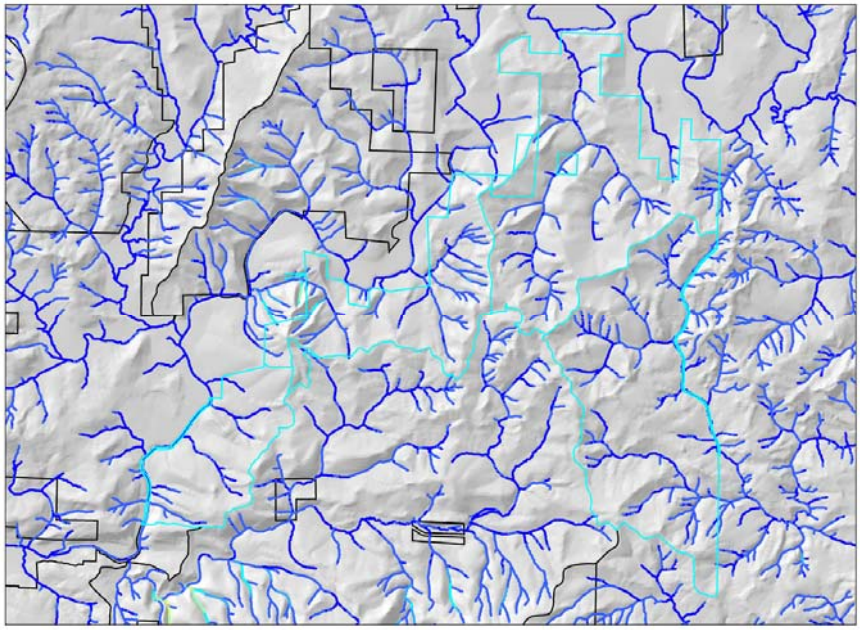

Figure D-34. Predicted debris flow probability for the Sager Management Basin. Refer to the Legend in Figure D-7. The predicted probabilities reflect cumulative landslide densities (that could trigger debris flows) and not individual pixel-based landslide potential shown in the landslide density map.

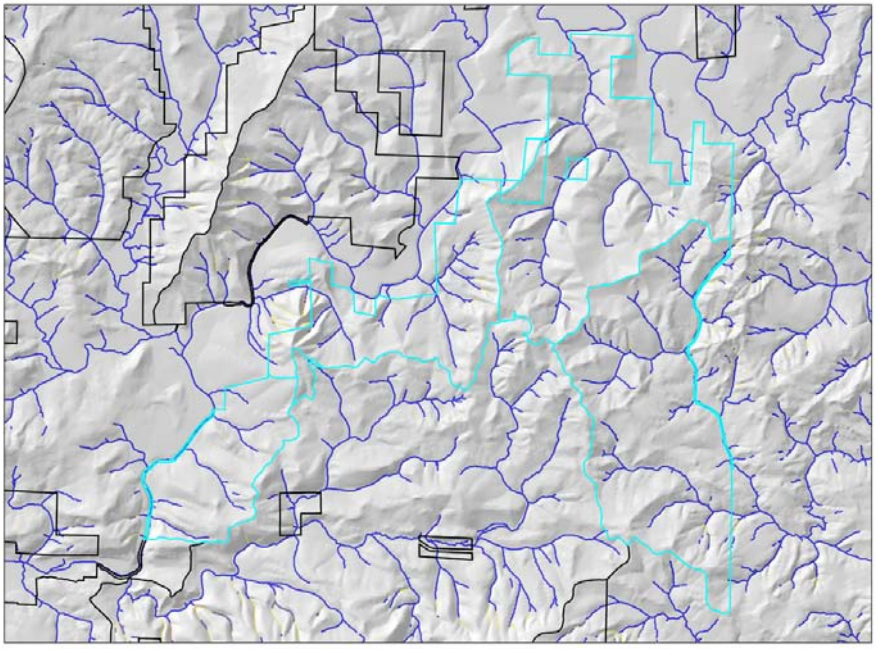

Figure D-35. Predicted headwater streams that contributed wood to fish-bearing channels by debris flows for the Sager Management Basin. Refer to the Legend in Figure D-7; predictions apply to headwater streams only. The predicted probabilities reflect cumulative landslide densities (that could trigger debris flows) and not individual pixel-based landslide potential shown in the landslide density map.

## 12. BUSTER MANAGEMENT BASIN

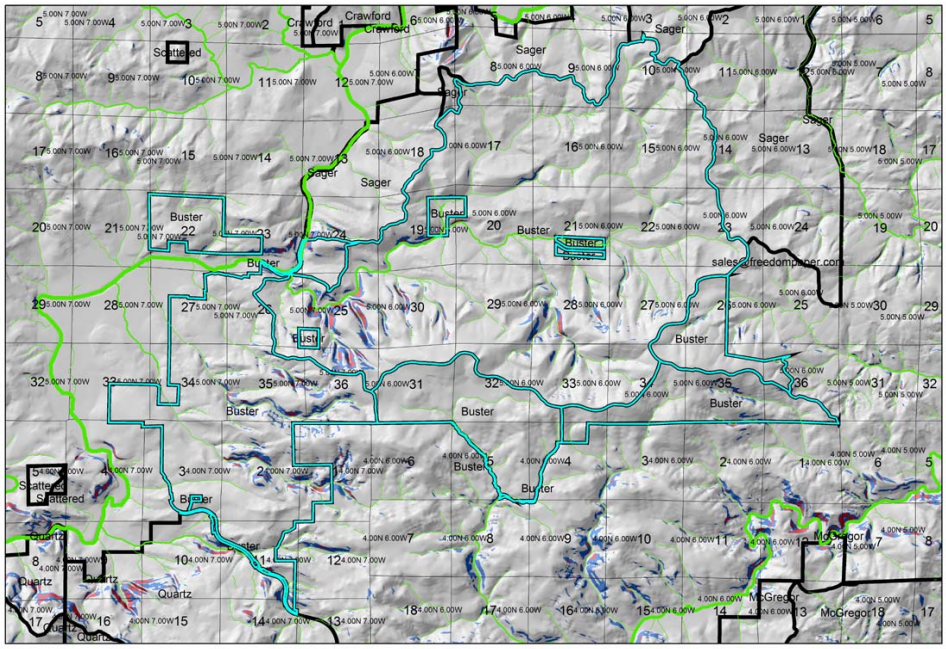


Figure D-36. Slope gradient map for the Buster Management Basin. Refer to the Legend in Figure D-7.

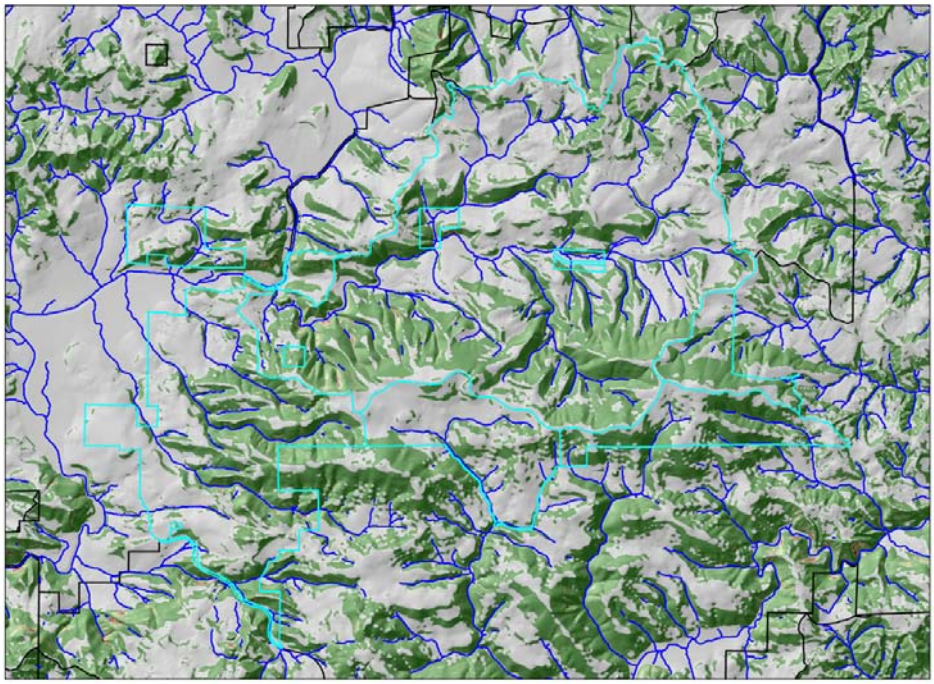

Figure D-37. Predicted landslide density for the Buster Management Basin. Refer to the Legend in Figure D-7; the gray areas have no predicted landslide density.

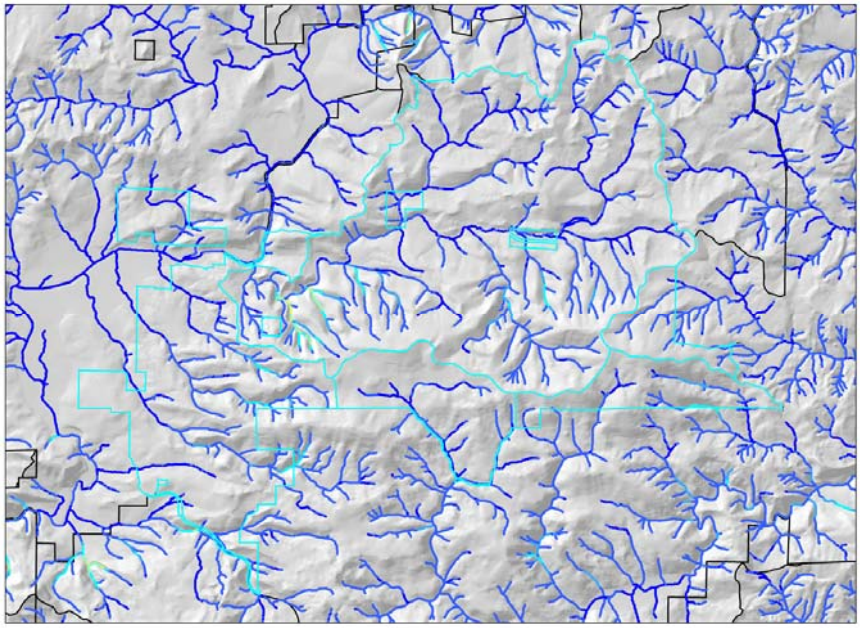

Figure D-38. Predicted debris flow probability for the Buster Management Basin. Refer to the Legend in Figure D-7. The predicted probabilities reflect cumulative landslide densities (that could trigger debris flows) and not individual pixel-based landslide potential shown in the landslide density map.

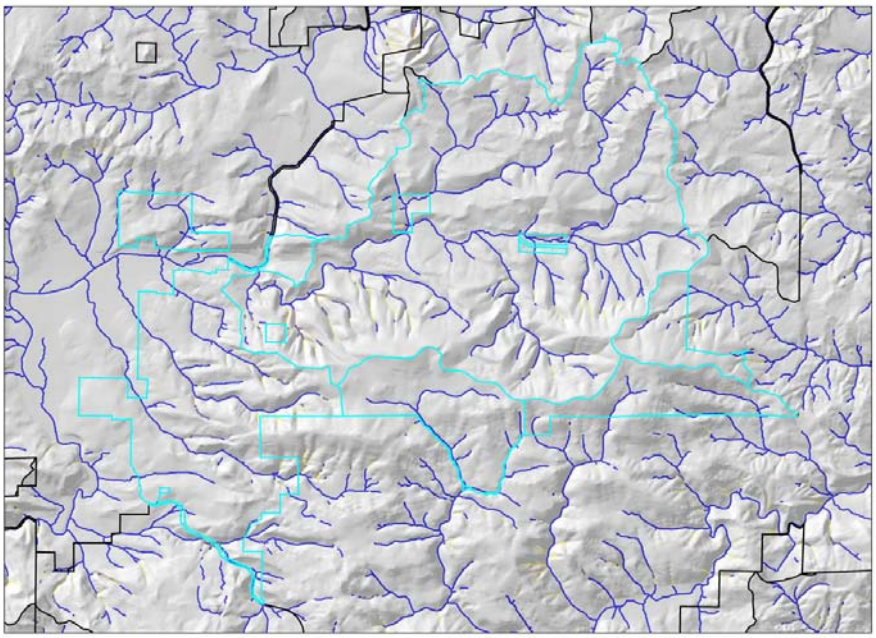

Figure D-39. Predicted headwater streams that contributed wood to fish-bearing channels by debris flows for the Buster Management Basin. Refer to the Legend in Figure D-7; predictions apply to headwater streams only. The predicted probabilities reflect cumulative landslide densities (that could trigger debris flows) and not individual pixel-based landslide potential shown in the landslide density map.

## 13. QUARTZ MANAGEMENT BASIN

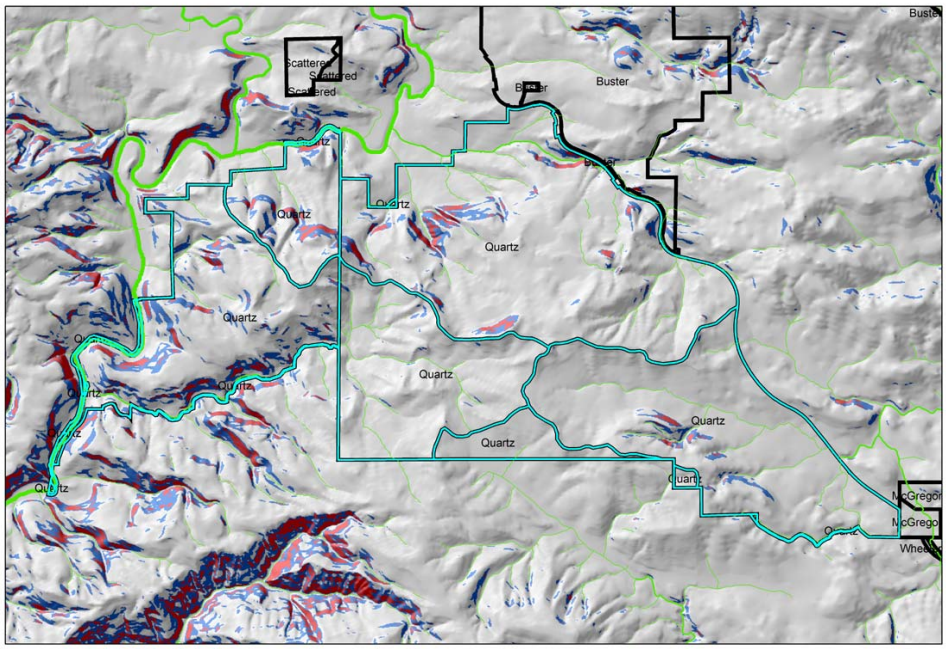


Figure D-40. Slope gradient map for the Quartz Management Basin. Refer to the Legend in Figure D-7.

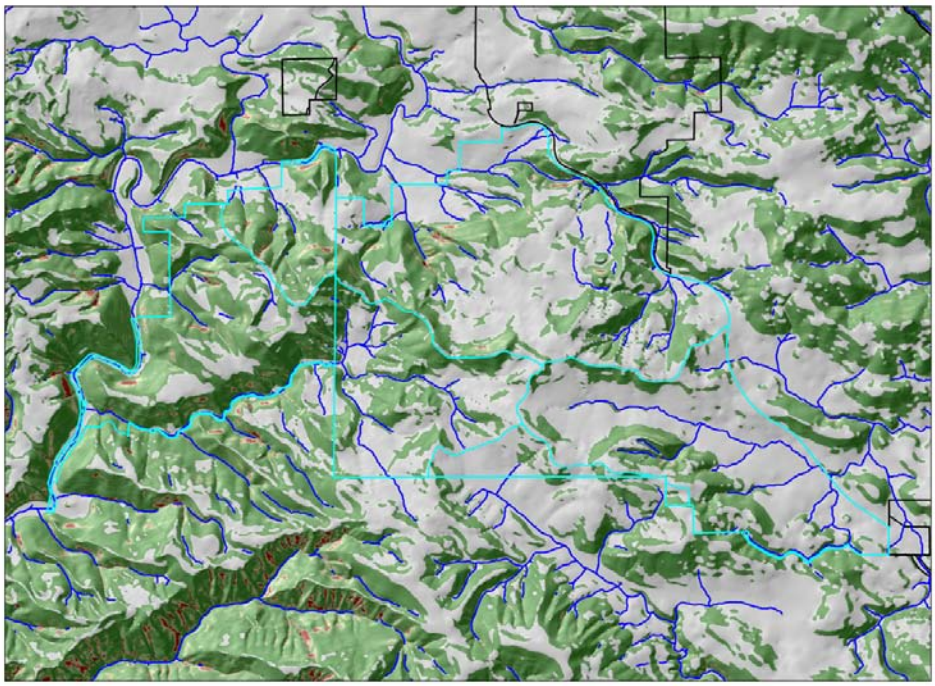

Figure D-41. Predicted landslide density for the Quartz Management Basin. Refer to the Legend in Figure D-7; the gray areas have no predicted landslide density.

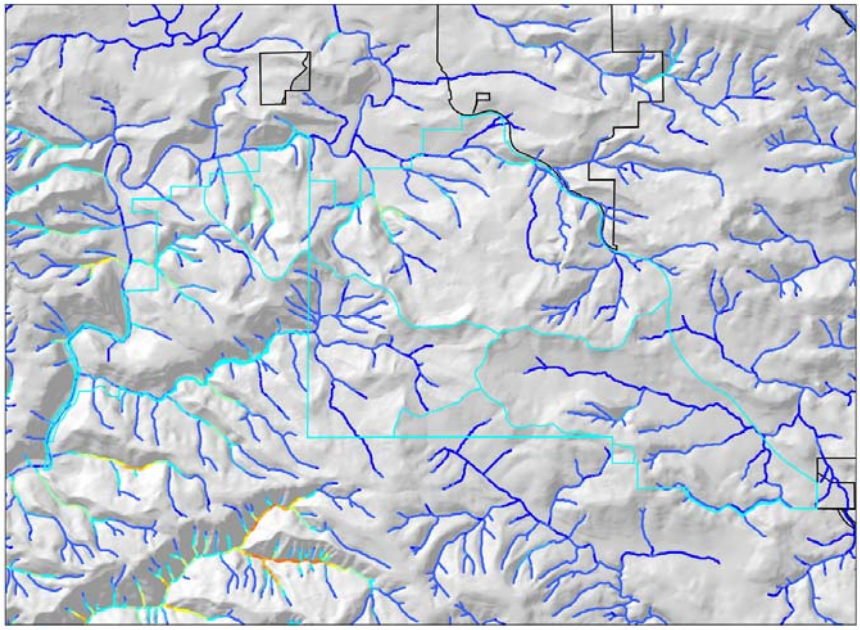

Figure D-42. Predicted debris flow probability for the Quartz Management Basin. Refer to the Legend in Figure D-7. The predicted probabilities reflect cumulative landslide densities (that could trigger debris flows) and not individual pixel-based landslide potential shown in the landslide density map.

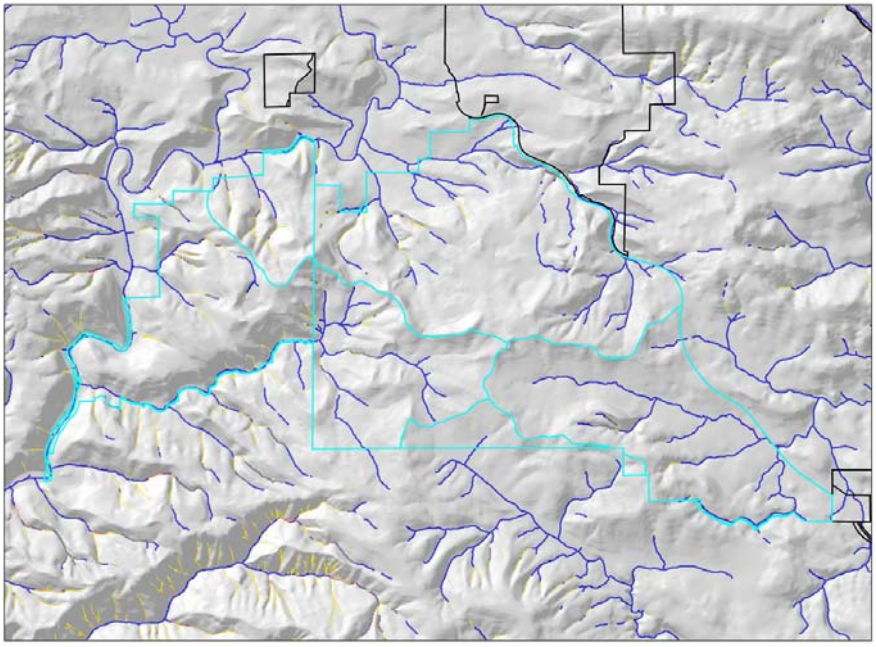

Figure D-43. Predicted headwater streams that contributed wood to fish-bearing channels by debris flows for the Quartz Management Basin. Refer to the Legend in Figure D-7; predictions apply to headwater streams only. The predicted probabilities reflect cumulative landslide densities (that could trigger debris flows) and not individual pixel-based landslide potential shown in the landslide density map.

## WILARK MANAGEMENT BASIN

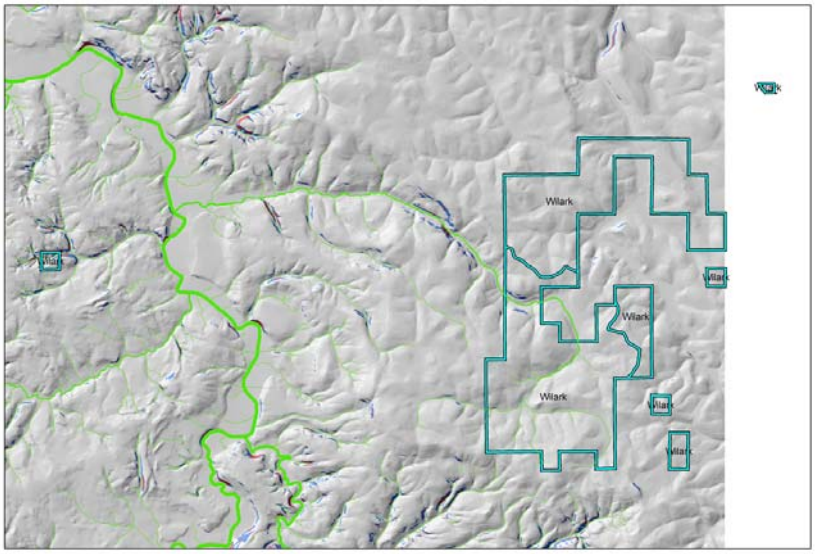


Figure D-44. Slope gradient map for the Wilark Management Basin. Refer to the Legend in Figure D-7.

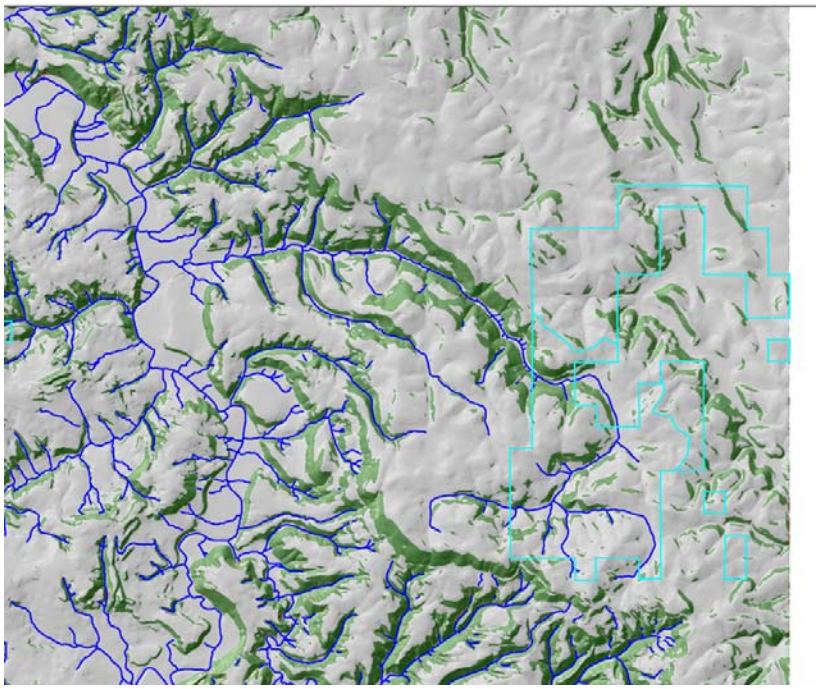

Figure D-45. Predicted landslide density for the Wilark Management Basin. Refer to the Legend in Figure D-7; the gray areas have no predicted landslide density. The predicted probabilities reflect cumulative landslide densities (that could trigger debris flows) and not individual pixel-based landslide potential shown in the landslide density map.

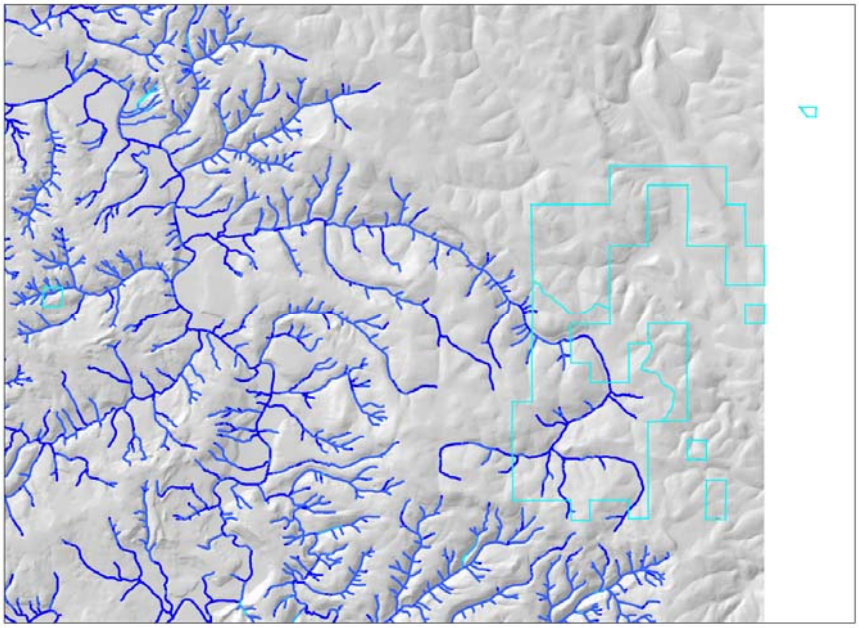

Figure D-46. Predicted debris flow probability for the Wilark Management Basin. Refer to the Legend in Figure D-7. The predicted probabilities reflect cumulative landslide densities (that could trigger debris flows) and not individual pixel-based landslide potential shown in the landslide density map.

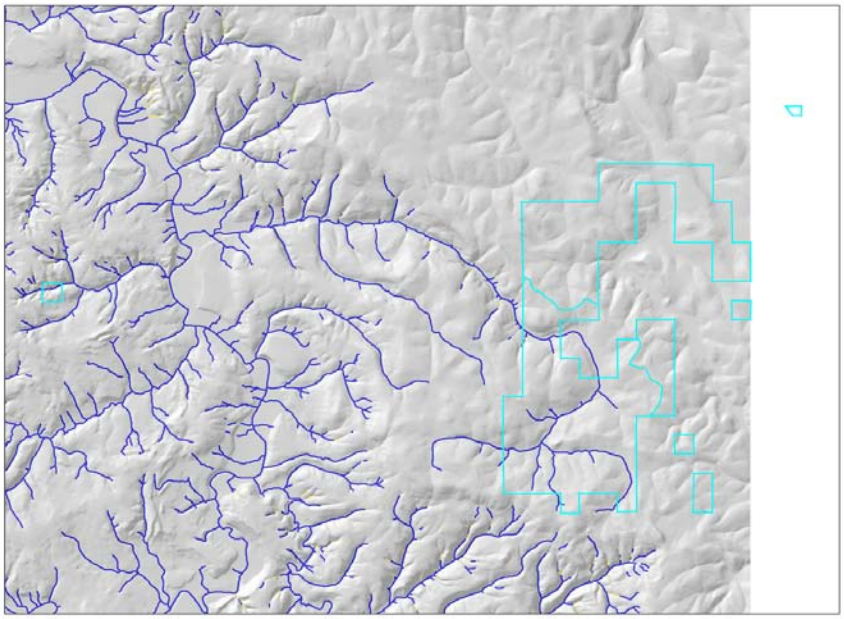

Figure D-47. Predicted headwater streams that contributed wood to fish-bearing channels by debris flows for the Wilark Management Basin. Refer to the Legend in Figure D-7; predictions apply to headwater streams only. The predicted probabilities reflect cumulative landslide densities (that could trigger debris flows) and not individual pixel-based landslide potential shown in the landslide density map.

## 14. MCGREGOR MANAGEMENT BASIN

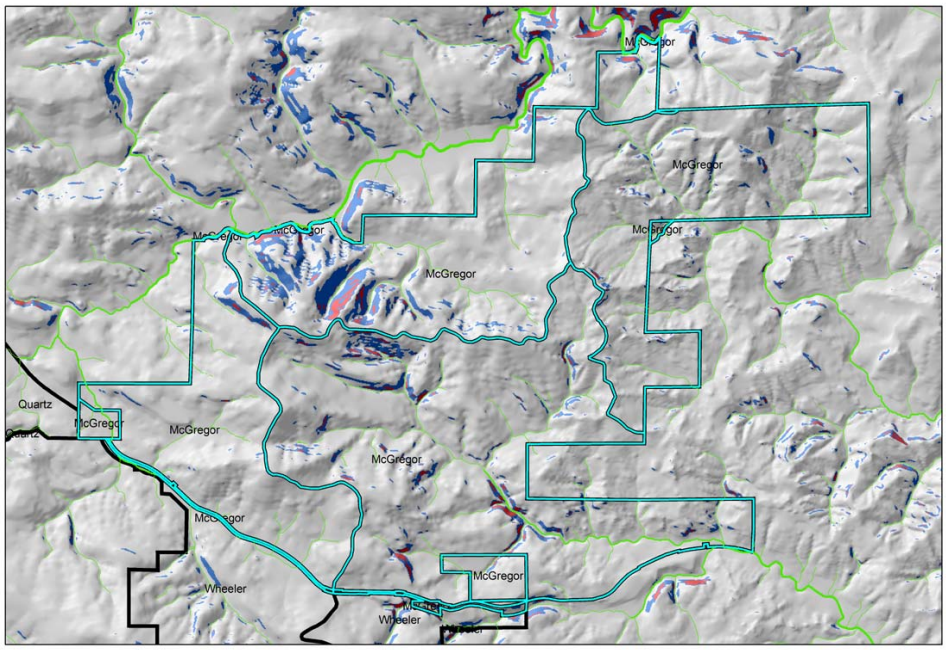


Figure D-48. Slope gradient map for the McGregor Management Basin. Refer to the Legend in Figure D-7.

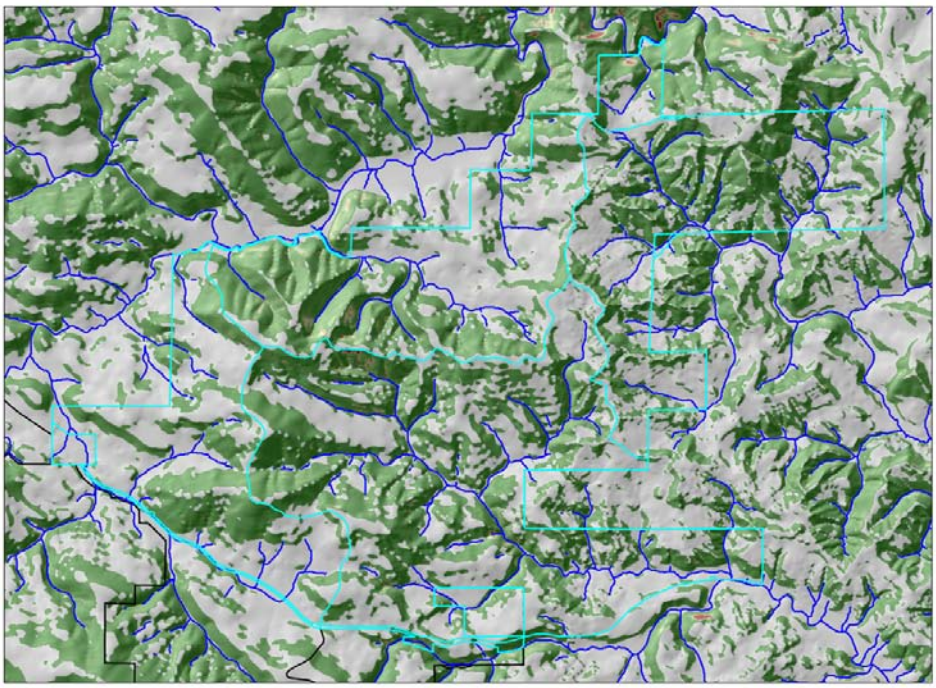

Figure D-49. Predicted landslide density for the McGregor Management Basin. Refer to the Legend in Figure D-7; the gray areas have no predicted landslide density.

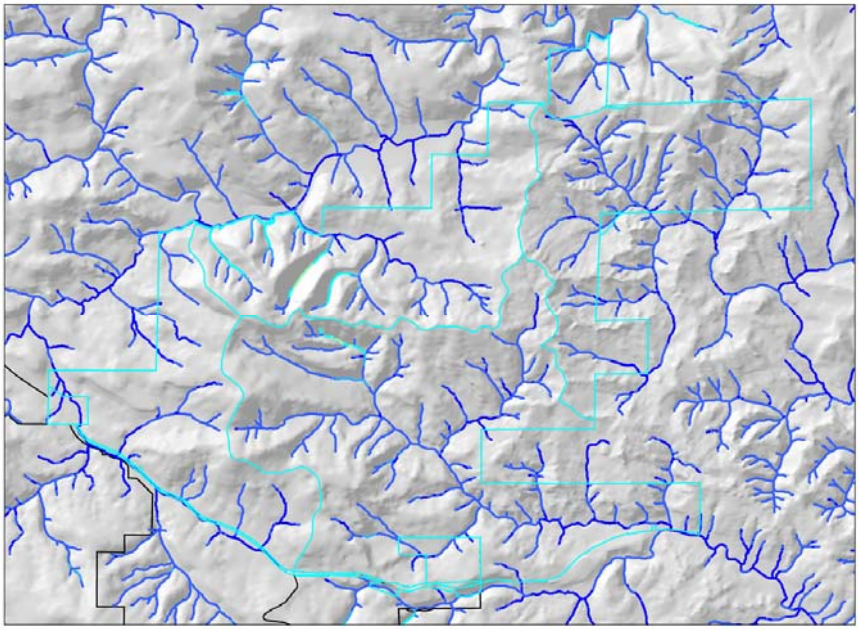

Figure D-50. Predicted debris flow probability for the McGregor Management Basin. Refer to the Legend in Figure D-7. The predicted probabilities reflect cumulative landslide densities (that could trigger debris flows) and not individual pixel-based landslide potential shown in the landslide density map.

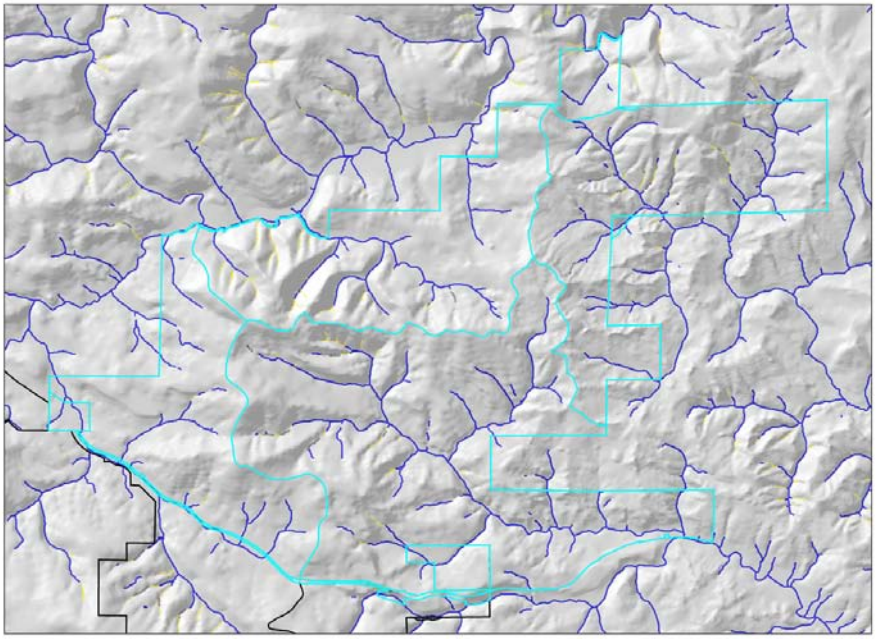

Figure D-51. Predicted headwater streams that contributed wood to fish-bearing channels by debris flows for the McGregor Management Basin. Refer to the Legend in Figure D-7; predictions apply to headwater streams only. The predicted probabilities reflect cumulative landslide densities (that could trigger debris flows) and not individual pixel-based landslide potential shown in the landslide density map.

## 15. WHEELER MANAGEMENT BASIN

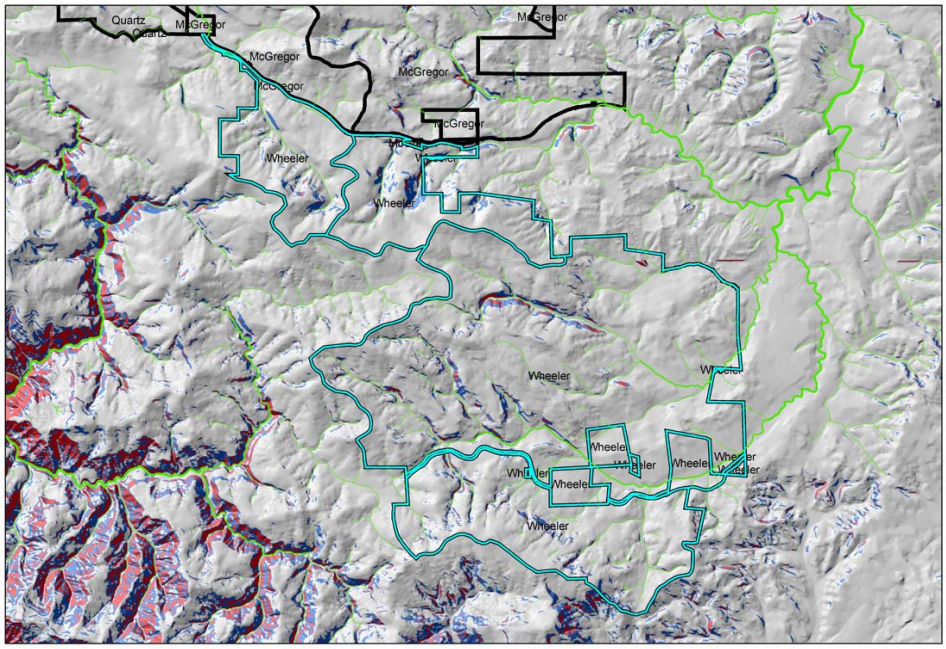


Figure D-52. Slope gradient map for the Wheeler Management Basin. Refer to the Legend in Figure D-7.

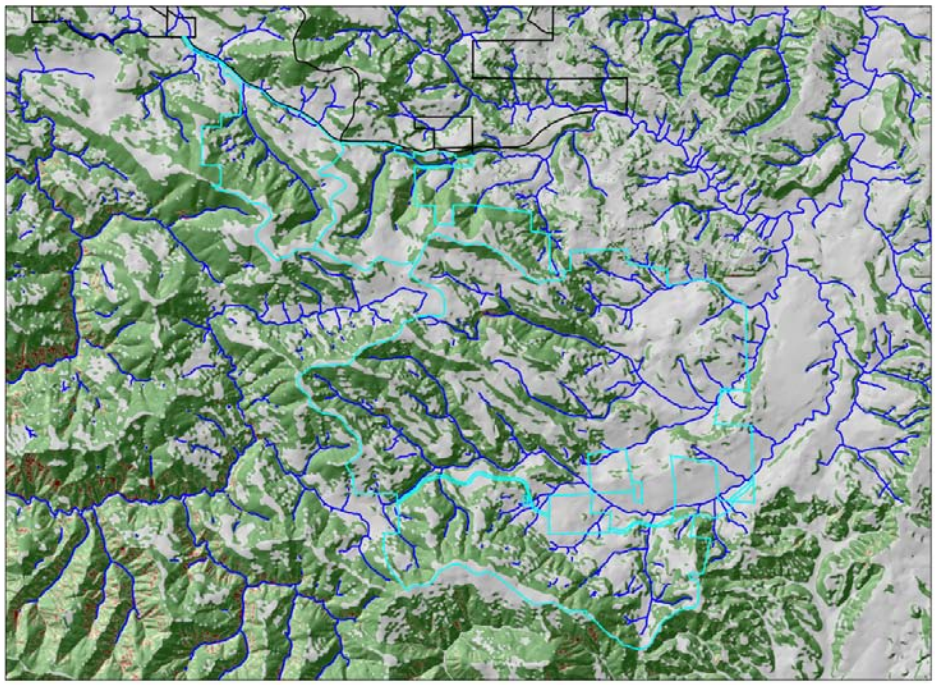

Figure D-53. Predicted landslide density for the Wheeler Management Basin. Refer to the Legend in Figure D-7; the gray areas have no predicted landslide density.

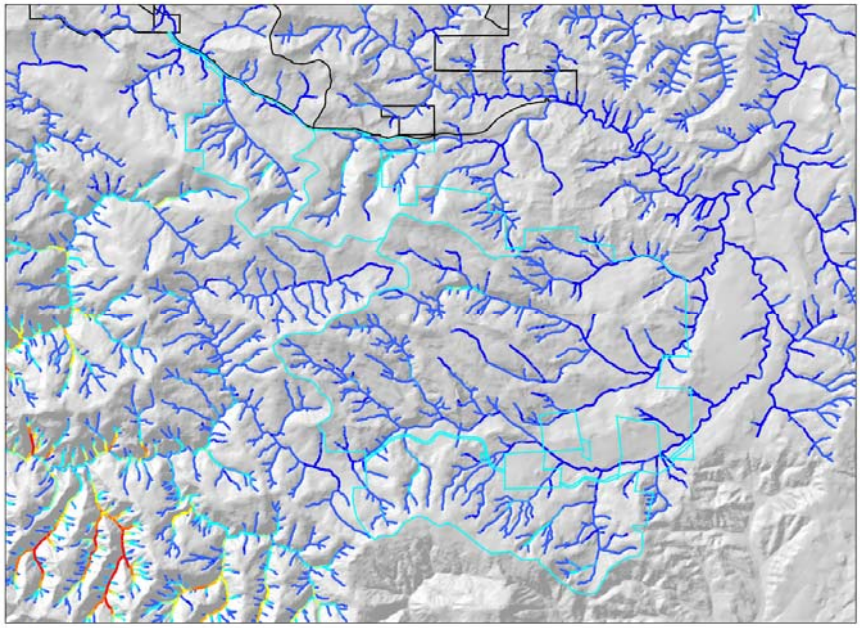

Figure D-54. Predicted debris flow probability for the Wheeler Management Basin. Refer to the Legend in Figure D-7. The predicted probabilities reflect cumulative landslide densities (that could trigger debris flows) and not individual pixel-based landslide potential shown in the landslide density map.

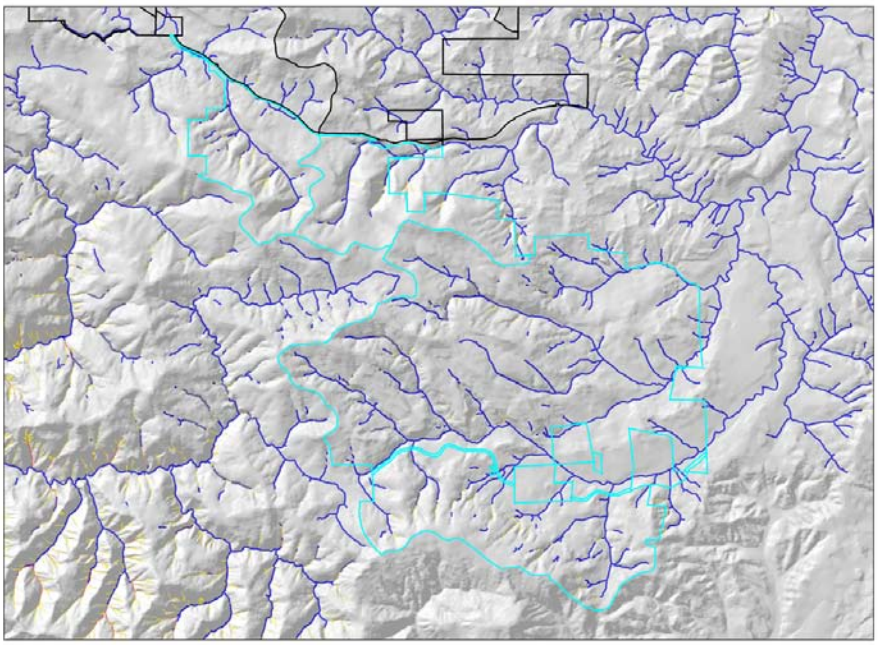

Figure D-55. Predicted headwater streams that contributed wood to fish-bearing channels by debris flows for the Wheeler Management Basin. Refer to the Legend in Figure D-7; predictions apply to headwater streams only. The predicted probabilities reflect cumulative landslide densities (that could trigger debris flows) and not individual pixel-based landslide potential shown in the landslide density map.

## 16. OTHER CONTIGUOUS PARCELS

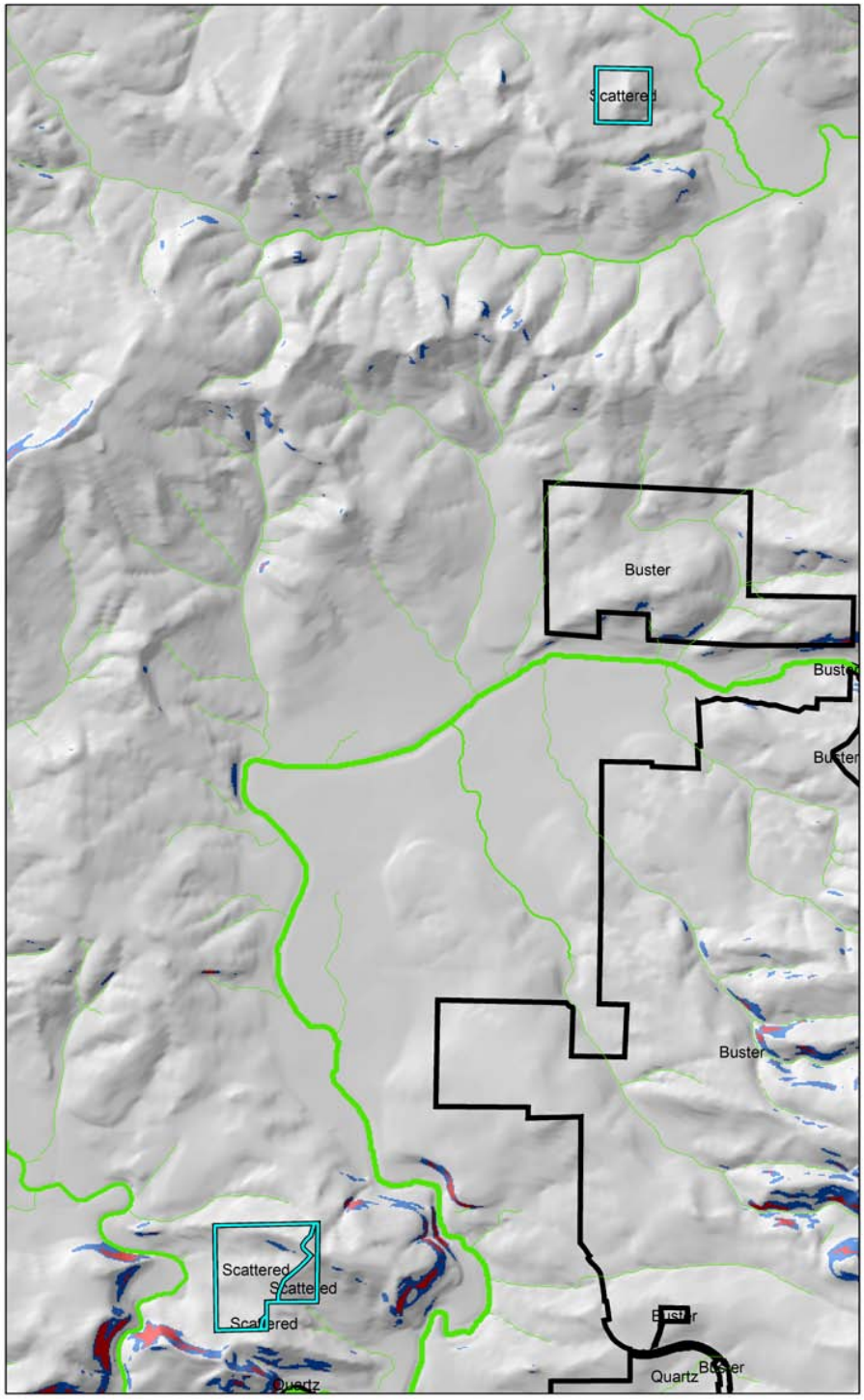


Figure D-56. Slope gradient map. Refer to the Legend in Figure D-7.

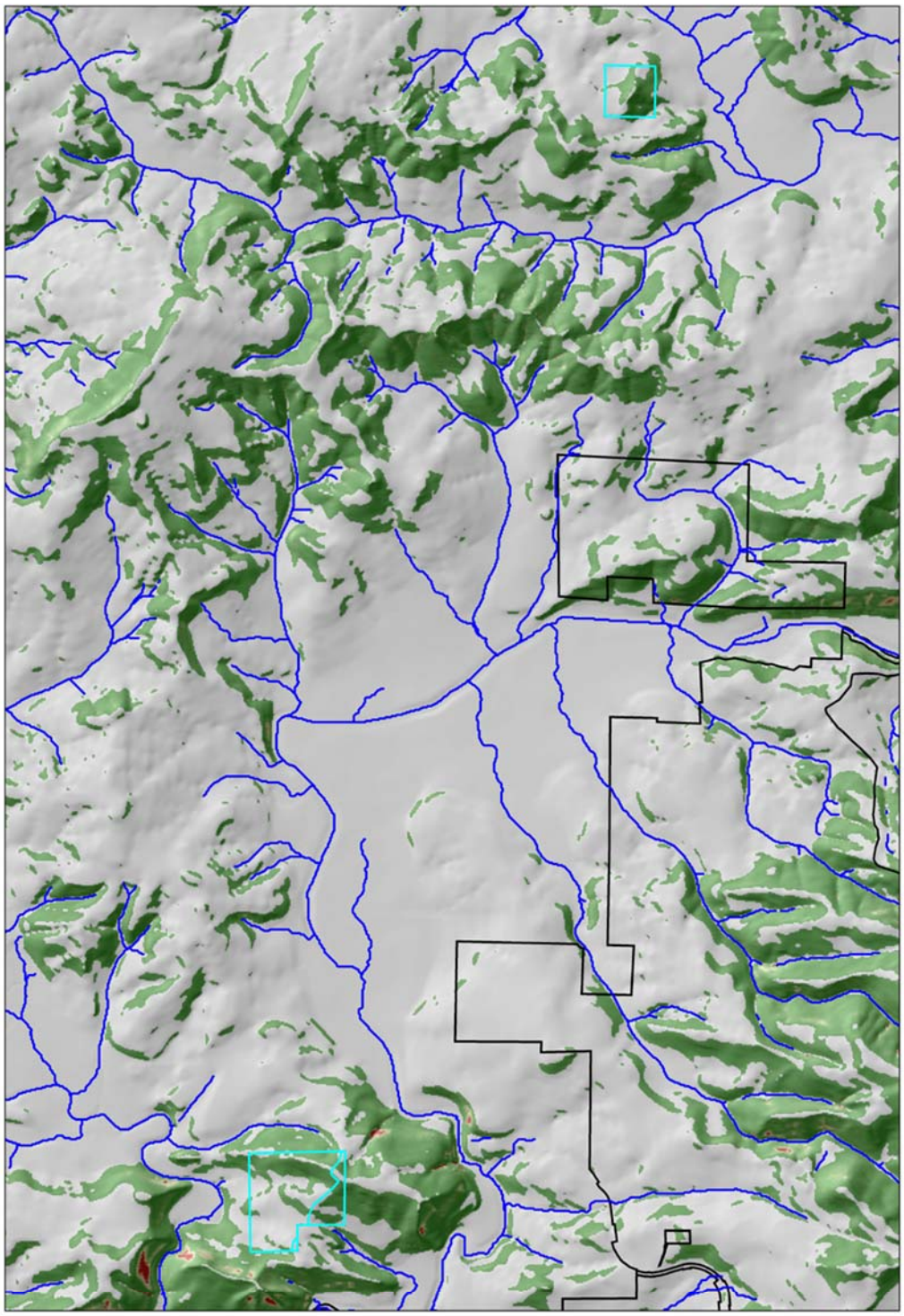

Figure D-57. Predicted landslide density. Refer to the Legend in Figure D-7; the gray areas have no predicted landslide density.

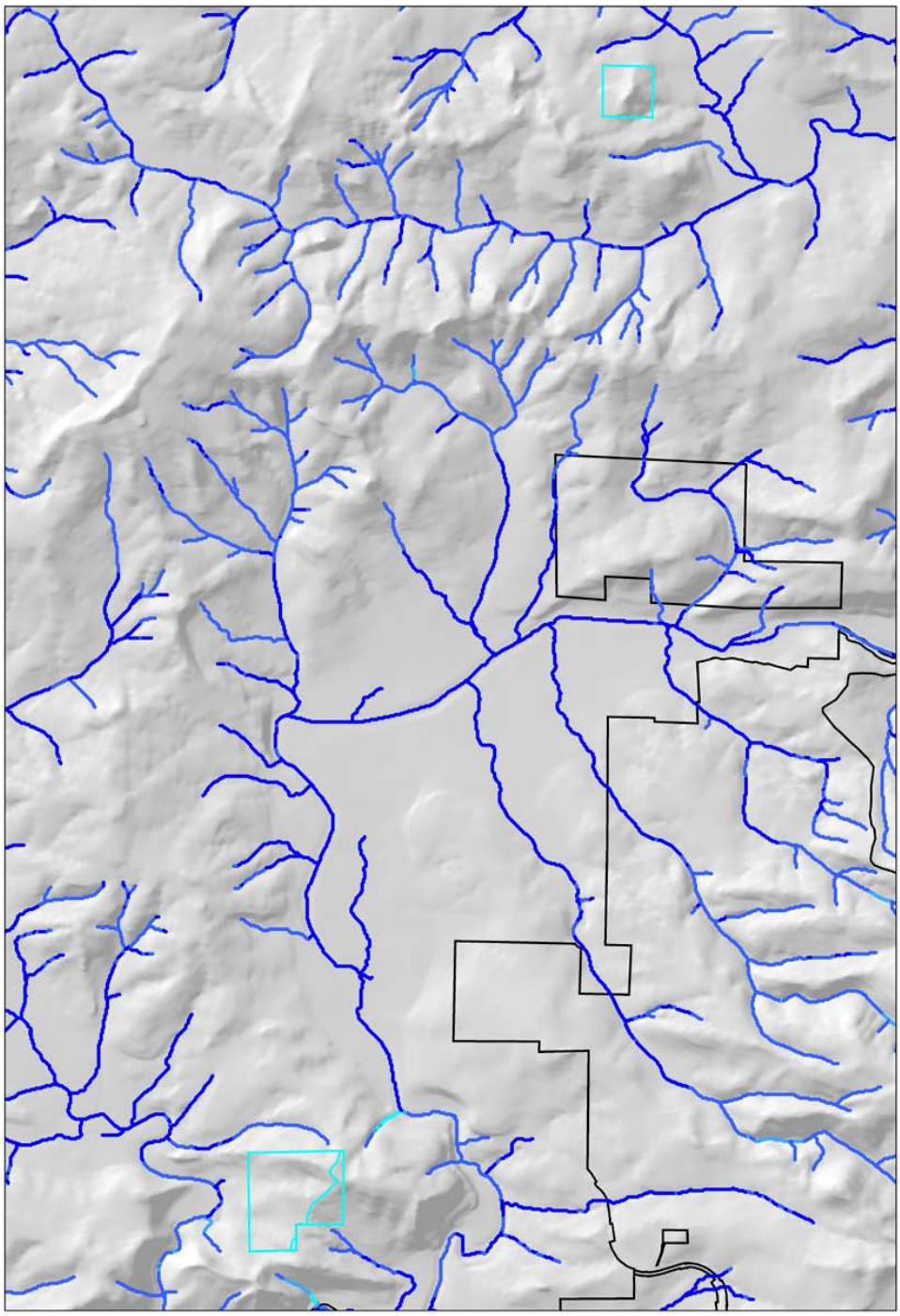

Figure D-58. Predicted debris flow probability. Refer to the Legend in Figure D-7. The predicted probabilities reflect cumulative landslide densities (that could trigger debris flows) and not individual pixel-based landslide potential shown in the landslide density map.

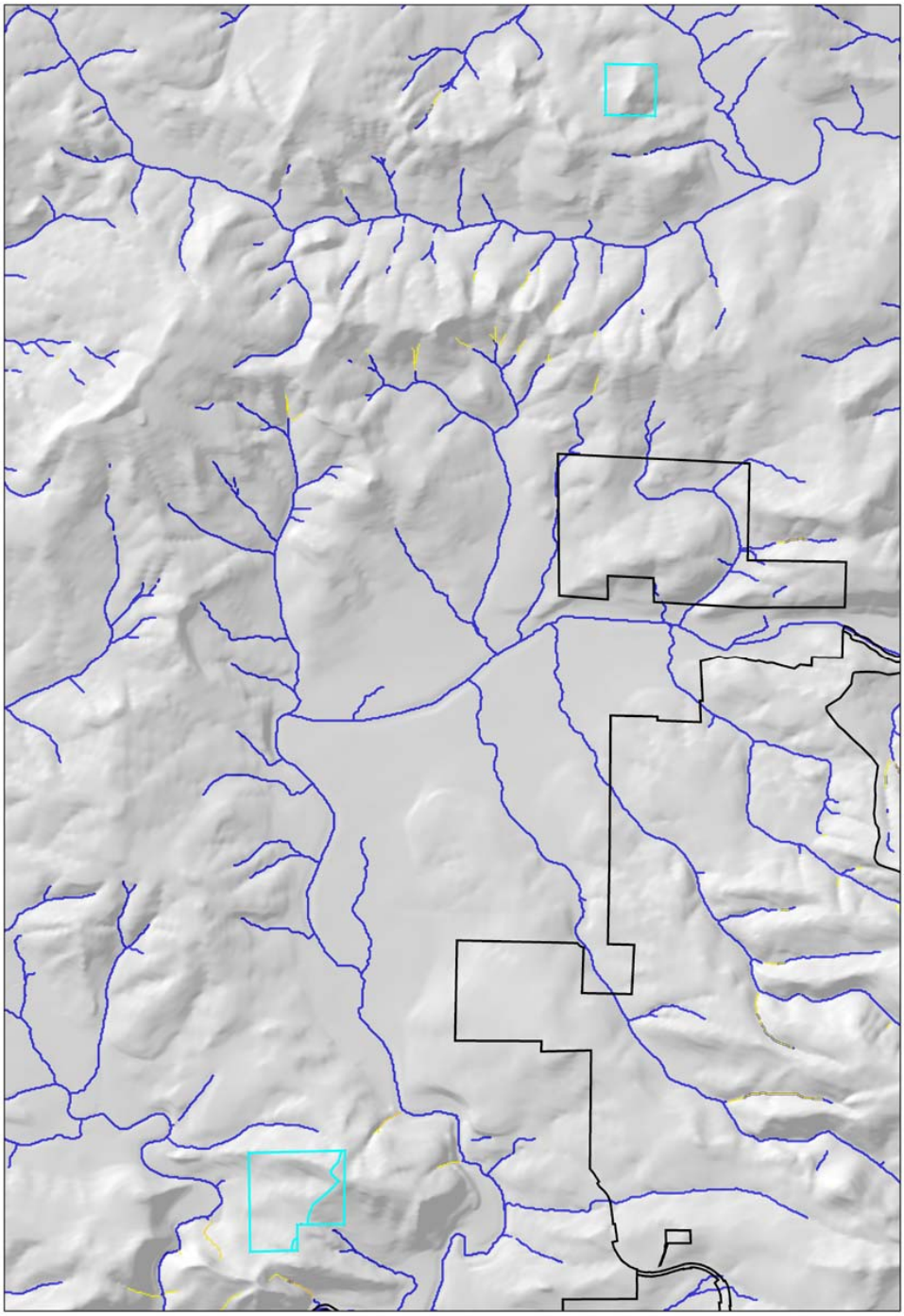

Figure D-59. Predicted headwater streams that contributed wood to fish-bearing channels by debris flows. Refer to the Legend in Figure D-7; predictions apply to headwater streams only. The predicted probabilities reflect cumulative landslide densities (that could trigger debris flows) and not individual pixel-based landslide potential shown in the landslide density map.

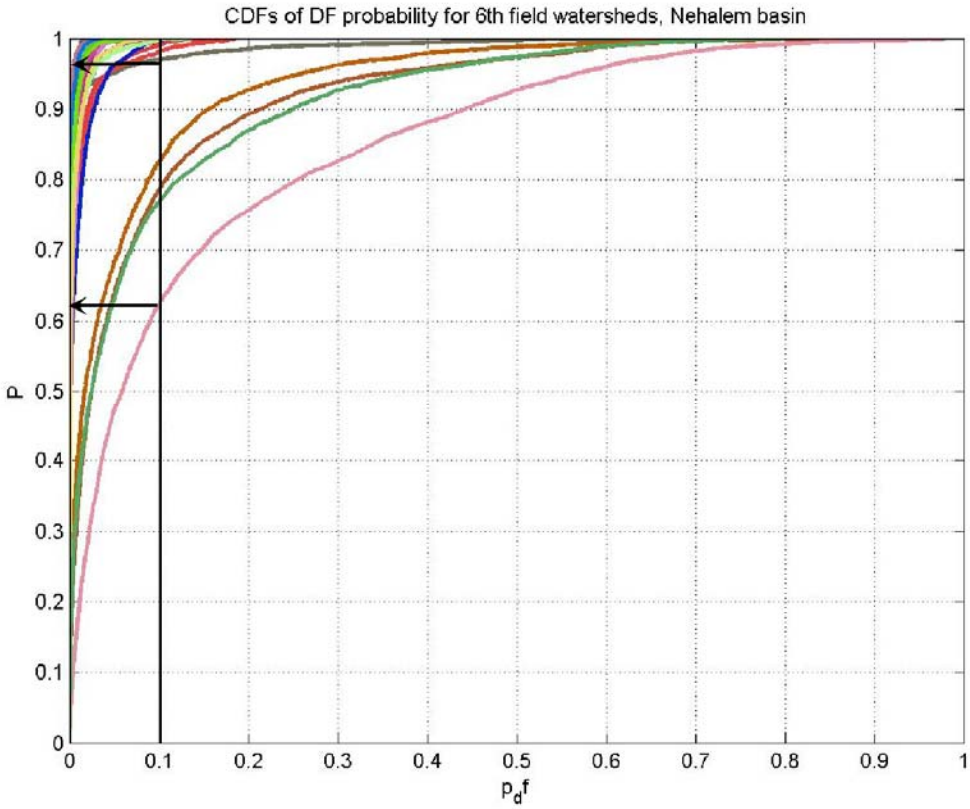


Figure D-60. The cumulative distribution of debris flow probabilities at the HUC 6th field watersheds in the Nehalem project area showing variation in the proportion of channels predicted to have greater than 10% probability (of a debris flow).

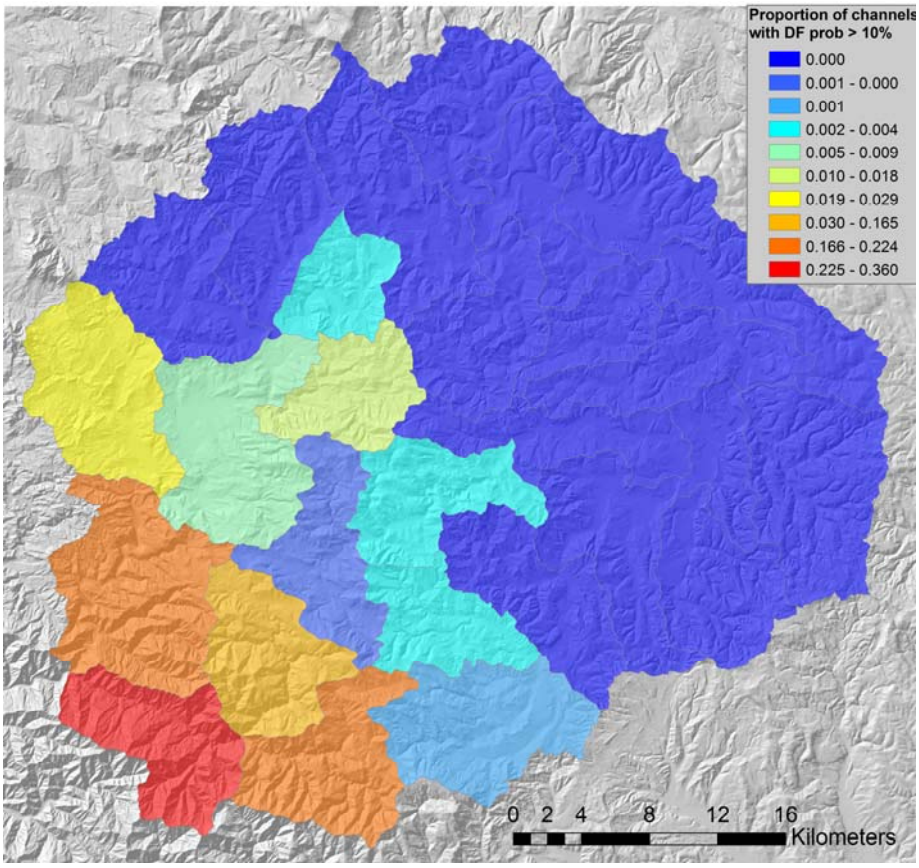


Figure D-61. The relative differences in the potential for debris flows in headwater streams at the HUC 6th field watersheds in the project area based on a 10% threshold shown in Figure D-58.

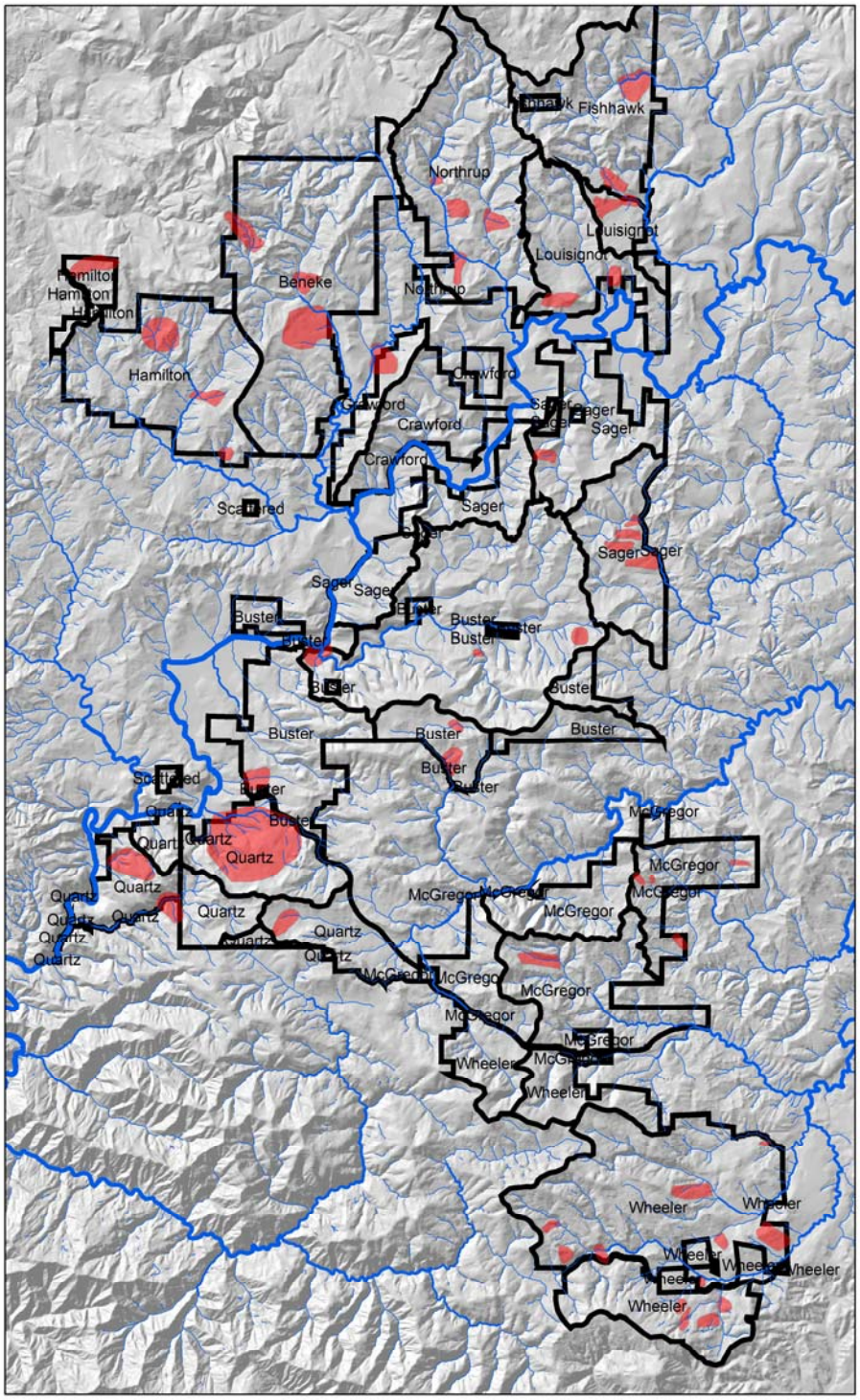


Figure D-62. A map of potential deep-seated landslides provided by the Oregon Department of Forestry (refer to Section 7.4.2 for methods).